ISBN: 978-628-96613-1-6. ISSN: 2414-6390. Digital Object Identifier: https://dx.doi.org/10.18687/LACCEI2025.1.1.2024

Mechanochemical Ligand Substitution in HKUST-1: Defect-Driven Enhancement of Hydrogen Storage Performance

Pablo S. Gauna[1,2]; Deicy Barrera[3]
[1]Universidad Tecnológica Nacional, Facultad Regional Delta, Argentina, *pgauna@campus.ungs.edu.ar*
[2]Universidad Nacional de General Sarmiento, Argentina
[3]Laboratorio de Sólidos Porosos (INFAP/ UNSL-CONICET), San Luis, Argentina, *deicybarrera@gmail.com*

***Abstract*– Hydrogen storage remains a major challenge due to its inherently low energy density (0.01 MJ/L compared to 34 MJ/L for gasoline), requiring compression for practical applications. Conventional storage methods (e.g., compression, liquefaction) present significant drawbacks, including safety concerns and high energy costs. An alternative approach is storage in sorbent materials, where Metal-Organic Frameworks play a crucial role due to their tunable properties and chemical and thermal stability. Among these materials, HKUST-1, composed of copper dimers coordinated with 1,3,5-benzenetricarboxylic acid, has emerged as a promising candidate, prompting extensive research into strategies for enhancing its storage performance.**

***This study investigates the effect of structural modifications in HKUST-1 on its adsorption behavior through a mixed-ligand approach. Three novel materials were synthesized with varying ligand ratios and characterized using nuclear magnetic resonance to determine their composition, powder X-ray diffraction and scanning electron microscopy for structural analysis, and thermogravimetric analysis to assess thermal stability. Additionally, textural properties were evaluated from nitrogen adsorption-desorption isotherms at 77 K, while hydrogen uptake experiments were conducted at 77 K up to 8 bar.**

One of the modified materials exhibited a remarkable 78% increase in H_2 uptake compared to HKUST-1, which is attributed to changes in the coordination environment of copper. Furthermore, although the original framework was preserved, a slight reduction in structural stability was observed. These findings highlight the potential of ligand substitution as an effective strategy for enhancing MOF-based hydrogen storage materials.

Keywords—Hydrogen, MOFs, HKUST-1, adsorption, mechanochemical synthesis.

I. Introduction

Hydrogen storage remains a fundamental challenge in the development of hydrogen-based energy technologies. At standard temperature and pressure (STP, 1 bar, 273.15 K), hydrogen exhibits an exceptionally low energy density of only 0.01 MJ/L [1], in stark contrast to gasoline, MJ/L [2]. To achieve practical storage densities, hydrogen must be compressed; however, conventional storage methods, including compression and liquefaction, face significant technical and economic barriers, such as safety concerns, high energy consumption, and efficiency losses[3], [4], [5].

An alternative and promising hydrogen storage strategy involves adsorption-based storage in porous materials, particularly Metal- Organic Frameworks (MOFs). These materials offer reversible, physisorption-driven hydrogen uptake under moderate conditions, circumventing traditional storage techniques' limitations. MOFs are particularly well-suited for hydrogen storage due to their high surface area, tunable pore architectures, and chemically tailorable metal centers that enhance H_2 adsorption. Unlike high-pressure tanks, which require costly infrastructure and pore risks of leakage, MOFs can safely store hydrogen at lower pressures, maintaining practical storage capacities while improving safety and efficiency [6].

Among MOFs, HKUST-1 has garnered significant interest as one of the most extensively studied materials for H_2 storage. This framework was first synthesized in 1999 at the *Hong Kong University of Science and Technology*, from which its name is derived. Structurally, HKUST-1 crystallizes in the cubic space group ***Fm3m*** and features a highly stable paddlewheel (PW) motif, which self-assembles into a three-dimensional porous network (Fig.1).

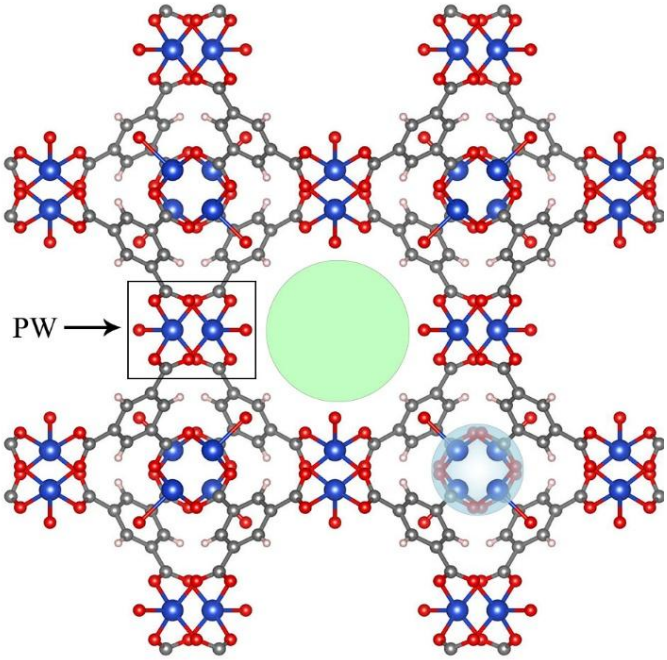

Fig. 1 Crystal structure of HKUST-1 visualized using VESTA [7]. The 3D PW network features pore channels (~1 nm, green circle) and pocket pores (~0.5 nm, light blue circle). Atoms: Cu (blue), O (red), C (gray), H (white).

The PW motif consists of a dinuclear copper (II) cluster, where each copper ion is coordinated equatorially by four carboxylate groups from 1,3,5-benzenetricarboxylic acid (BTC) ligands, , forming a rigid
square-planar geometry around the Cu^{2+} ions. The axial positions in the coordination sphere are completed by two water molecules [8].

The repeating arrangement of PW unit generates a highly porous structure with channels approximately 1 nm in diameter (Fig. 1, green circle). Additionally, smaller pocket-type pores (~0.50 nm, Fig. 1, blue circle) connect to these channels via windows of 0.35 nm [9]

A key structural feature of HKUST-1 is the presence of open metal sites (OMS), which play a critical role in gas adsorption. These highly reactive coordination sites emerge upon the thermal or vacuum-induced removal of coordinated water molecules, leaving behind undercoordinated copper centers capable of interacting strongly with adsorbates [10].

OMS exhibit notable interactions with polar gases, such as hydrogen, via electrostatic forces, enhancing adsorption capacity. The strength of these interactions depends on the gas's quadrupole moment and the electronic properties of exposed metal centers [11], [12].

This ability to selectively adsorb gases positions HKUST-1 as a compelling candidate for hydrogen storage applications. However, optimizing H_2 uptake requires structural modifications to balance porosity, stability, and host-guest interactions.

Both theoretical models and experimental evidence suggest that enhancing the number of OMS in HKUST-1 is feasible by modifying the copper coordination environment via ligand substitution. A mixed-ligand approach, which involves partially replacing BTC ligands during synthesis, has been explored as a strategy to tailor the adsorption properties of HKUST-1 [13], [14], [15].

However, traditional solvothermal synthesis, the standard method for ligand substitution, poses major challenges, including high solvent toxicity and substantial energy consumption, requiring the development of greener alternatives[16]. Mechanochemistry, a solvent-free synthesis technique, has emerged as a green and energy-efficient method for MOF engineering. This approach not only reduces environmental impact but also allows for precise control over defect generation and ligand substitution, thereby enhancing the material's performance and stability.

In this work, we investigate the mechanochemical mixed-ligand strategy by partially replacing BTC with 1,3-benzenedicarboxylic acid (iBDC) in HKUST-1, with the aim of improving hydrogen uptake capacity and optimizing adsorption behavior.

II. Experimental

A. Synthesis and activation

Four materials were synthesized using the mechanochemical method: HKUST-1 and three variants, denoted as *H-Mix-XX*, where "XX# represents the BTC percentage in the final solid.

The synthesis followed this procedure: 1.76 g (18 mmol) of copper (II) hydroxide (Sigma-Aldrich, technical grade, 55–56% purity) and a variable amount of ligands (Table 1)—BTC (Sigma-Aldrich, 95%) and iBDC (Sigma-Aldrich, 99%)—were dry-mixed in a mortar for 5 minutes. Then, 10 mL of absolute ethanol (Anedra, PA-ACS) was added, and mixing continued for another 10 minutes. The resulting solids were activated in methanol (Anedra, PA-ACS) for three days, replenishing solvent every 24 hours.

TABLE 1
AMOUNTS OF BTC AND IBDC USED FOR THE SYNTHESIS OF MATERIALS. THE VALUES ASSIGNED TO XX CORRESPOND TO THOSE DETERMINED BY NMR (SEE RESULTS AND DISCUSSION SECTION).

MOF	BTC (mmol)	iBDC (mmol)	% BTC (theoretical)	% BTC (measured)
HKUST-1	12.0	-	100	100
H-Mix-90	10.8	1.2	90	90
H-Mix-84	9.6	2.4	80	84
H-Mix-77	8.4	3.6	70	77

B. Nuclear magnetic resonance

Nuclear magnetic resonance (NMR) spectroscopy confirmed the presence of both ligands in the synthesized solids. The relative amount of each ligand in the MOFs was determined by integrating the peak areas.

NMR spectra were recorded on a Bruker UltraShield 14.1 Tesla spectrometer (^{1}H 600.13 MHz) equipped with a Bruker Smart Probe BBFO (5 mm) and a Bruker Avance III control and data acquisition system. For analysis, 5 mg of each sample was dissolved in 1 mL of deuterated trifluoroacetic acid.

C. Powder X ray diffraction

Powder X-ray diffraction (PXRD) was used to analyze the crystal structure by comparing the experimental patterns with the theoretical diffraction profile.

Measurements were performed on a Panalytical Empyrean diffractometer equipped with a PixCel3D detector in Bragg-Brentano configuration. The analysis used Cu Kα radiation (λ = 1.54056 Å) at 40 mA and 40 kV, over a 2θ range of 5–40°, with a step size of 0.026° and an acquisition time of 59 seconds per step.

D. Scanning electronic microscopy

Scanning electron microscopy (SEM) images were acquired using a Karl Zeiss FESEM DSM 982 Gemini microscope in emissive mode at 3.0 keV, equipped with an Everhart-Thornley detector. Before imaging, the samples were coated with a gold film.

E. Thermogravimetric analysis

Thermogravimetric analysis (TGA) determined the water loss and decomposition temperature in the different solids. The study used a TA Instruments SDT Q600 analyzer with an alumina sample holder coupled to a Discovery mass spectrometer (MS). The samples were heated under a nitrogen

atmosphere (Linde, 99.998% purity) from room temperature to 453 K at a heating rate of 10 K·min⁻¹, held under isothermal conditions for 180 minutes, and then heated up to 673 K at the same rate.

F. Isotherm determination and textural properties

The adsorption-desorption isotherms of the synthesized MOFs were measured using nitrogen (Linde, 99.998% purity) at 77 K on a Micromeritics ASAP 2000 manometric system. Before analysis, ~100 mg of each sample was degassed under vacuum (0.013 mbar) with a mechanical pump for 12 hours at 323 K. The temperature was then increased to 453 K at a rate of 1 K·min⁻¹ and held for 3 hours.

Textural properties were derived from the isotherm data. The specific surface area was calculated using the Rouquerol criteria [17], the micropore size was determined with the Dubinin–Radushkevich method [18], and the total pore volume was estimated using the Gurvich rule at $p/p^o = 0.98$ [12].

III. Results and Discussion

NMR spectra for the four materials are shown in Fig. 2. A peak at a chemical shift of approximately 9.2 ppm is observed. This is attributed to the three protons of BTC detected in this study (Fig. 3), as deduced from the spectrum of the pure ligand [19].

Additionally, the signals at 8.9, 8.5, and 7.7 ppm observed in Fig. 5.1b, 5.1c, and 5.1d indicate the presence of the three protons with their respective chemical environments from the iBDC ligand (Fig.) 3, according to the NMR spectrum of the pure compound [19].

Both the BTC and iBDC signals in the NMR spectra appeared significantly broader than those of the pure ligands. This broadening is attributed to the unpaired electron of the copper in the MOFs, which generate a variable-intensity magnetic field. The resulting rapid nuclear spin relaxation shortens the relaxation time, increasing the signal width, as these variables are inversely proportional [19].

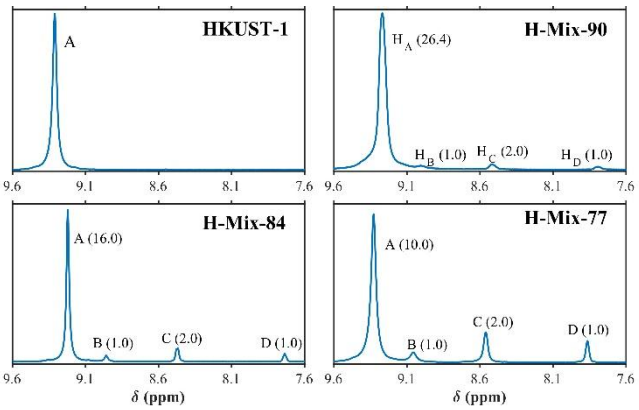

Fig. 2 NMR spectra of HKUST-1 and H-Mix-90/84. The values in parentheses represent the integrated peak areas for each proton

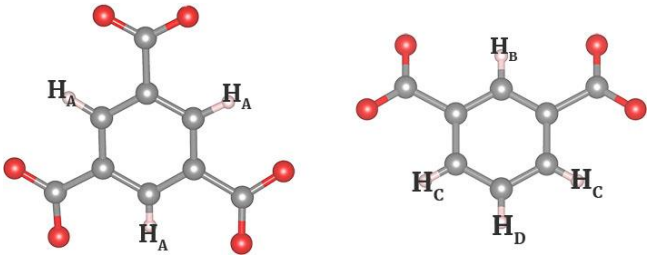

Fig. 3 Molecular structures of BTC (left) and iBDC (right) visualized using VESTA [7]. C atoms, gray; O atoms, red and H, white. Protons are labelled according to their chemical environments for identification and quantification by NMR.

The molar fraction of BTC in each MOF was then calculated using and calculating the molar fraction of BTC in each MOF using (1):

$$X_{BTC} = \frac{(1/3).area_{H_A}}{(1/3).area_{H_A}+(1/2).area_{H_C}} \quad (1)$$

where H_A corresponds to the three protons of BTC and H_C corresponds to the protons of iBDC (Fig 3). Since the latter represents only two protons, it introduces a lower error in the calculation.

The measured molar fraction was higher than the theoretical value. This discrepancy can be attributed to the increased tendency of BTC molecules to coordinate with copper, given that BTC contains an additional carboxylate group compared to iBDC. The results of the molar fraction calculations are presented in Table 1.

The PXRD patterns of all synthesized materials exhibit characteristic reflections (e.g., peaks in the diffraction patterns) corresponding to the parent HKUST-1 framework (Fig. 4), confirming the retention of its cubic structure even after partial ligand substitution. The preservation of key reflections (corresponding to diffraction crystallographic planes [200], [220] and [222]) indicates that the copper paddlewheel nodes—dimers of Cu^{2+} ions bridged by carboxylate groups from BTC ligands—remain intact, maintaining the framework's long-range order (e.g., periodic arrangement) despite replacing up to 23% of BTC.

This structural stability is consistent with prior studies showing that the paddlewheel architecture of HKUST-1 can tolerate ligand modifications without collapsing as long as the coordination geometry of the substituted ligands remains compatible with the original framework[20]. Subtle variations in peak intensities suggest localized electronic redistributions or strain induced by ligand mismatch [21], while progressive peak broadening at lower BTC fractions indicates increased crystallite size reduction [22].

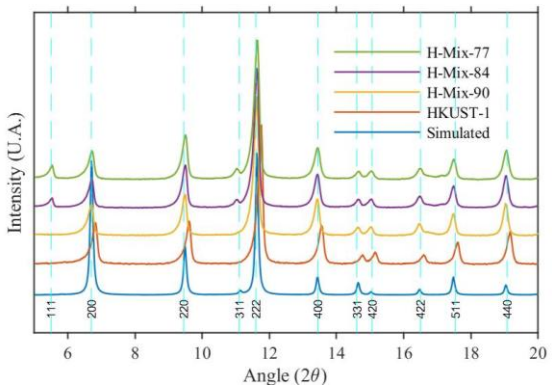

Fig 4 Diffraction patterns of simulated HKUST-1 mixed-ligand MOFs. Crystallographic planes are indicated below the first curve.

SEM images (Fig. 5) reveal distinct morphological changes across the series: H-Mix-90 exhibits amorphous-like aggregates, while H-Mix-84/77 display lamellar crystals. Despite these surface variations, PXRD confirms all materials retain the cubic HKUST-1 framework without additional reflections, which rules out bulk phase segregation.

The lamellar structures in H-Mix-84/77 likely arise from anisotropic growth templated by iBDC's linear geometry, reorganising surface layers without disrupting the underlying cubic lattice. This surface restructuring, coupled with preserved bulk crystallinity, highlights the potential to decouple morphological and structural properties in mechanochemical MOF design [21], [22].

TGA curves (Fig. 6) reveal that HKUST-1 has a water content of 12% (observed by the weight loss between 25 and 180°C and characterized by mass spectrometry), while the other solids exhibit a loss of about 19%. This difference might be because HKUST-1 has fewer available OMS, where water molecules can be strongly attracted due to their high dipole moment [23]. On the other hand, the decomposition temperature of the mixed-ligand MOFs is lower than that of HKUST-1 (343°C vs. 350°C), suggesting that the three-dimensional network loses some stability due to the defects introduced by ligand replacement [15].

The nitrogen adsorption-desorption isotherms at 77 K (Fig. 7) exhibit a hybrid shape between Type I and Type II according to IUPAC classification [24], which indicates hierarchical micro-mesoporous materials. The steep adsorption at low relative pressures ($p/p^o < 0.1$) corresponds to micropore filling, while the sharp uptake near saturation ($p/p^o \approx 1$) reflects capillary condensation in mesopores [24].

Textural properties derived from these isotherms (Table 2) reveal that mesopores account for 32% of the total pore volume in HKUST-1, whereas d H-1-Mix90/84/77, show lower mesoporosity (24%, 15%, and 18%, respectively).

Isotherm profiles are consistent with prior studies on HKUST-1 prepared via analogous methods, where specific surface up to 1700 m²/g was reported [25], [26], [27]. Which can be compared with the HKUST-1-Mix90 area of 1750 m²/g (Table 2).

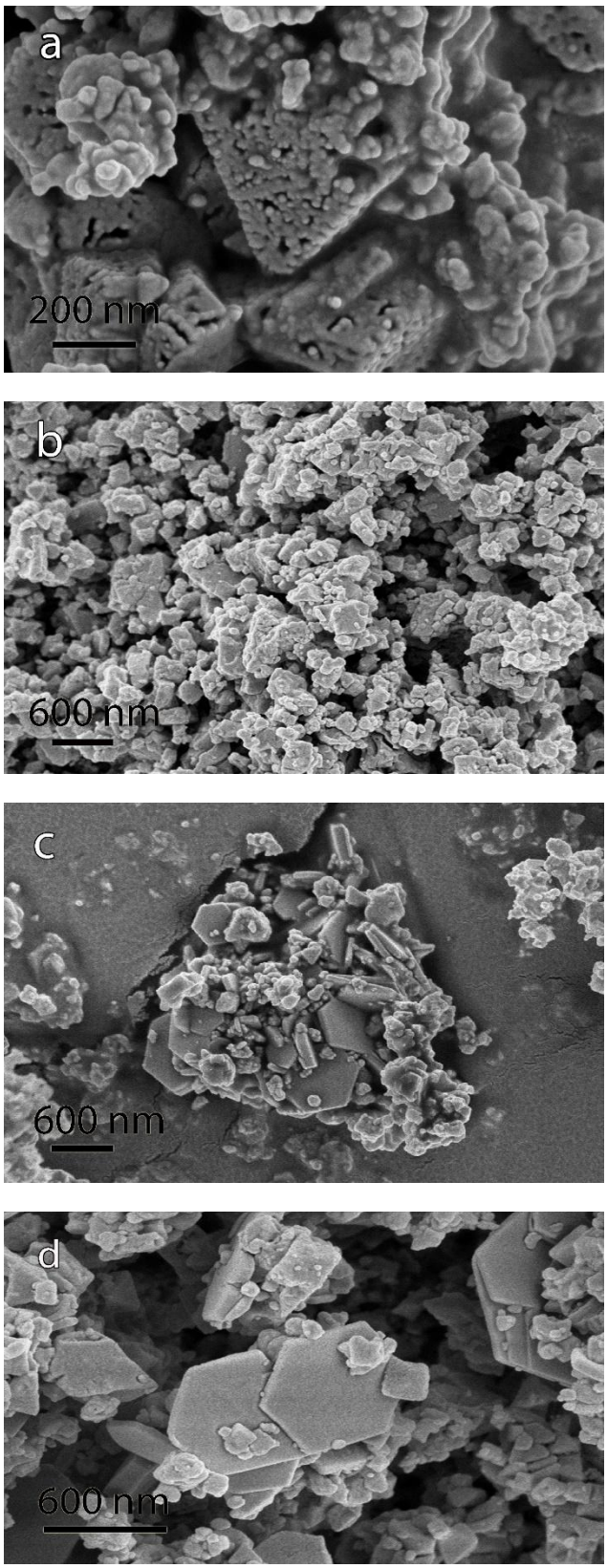

Fig. 5 SEM images for HKUST-1 (a), and H-Mix90/87/77 (b), (c),(d) respectively.

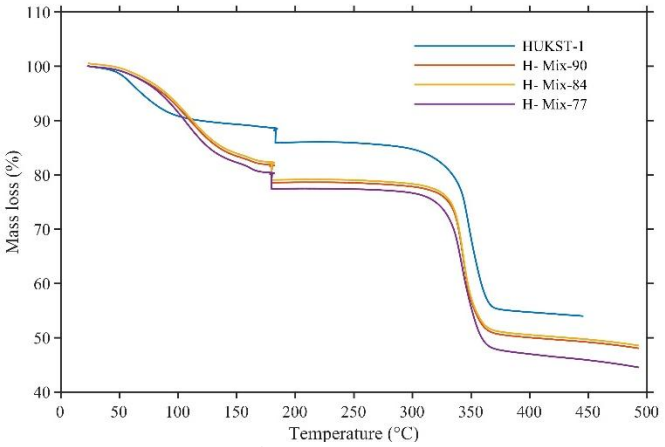

Fig. 6. TGA curves for HKUST-1 and H-Mix-XX MOFs

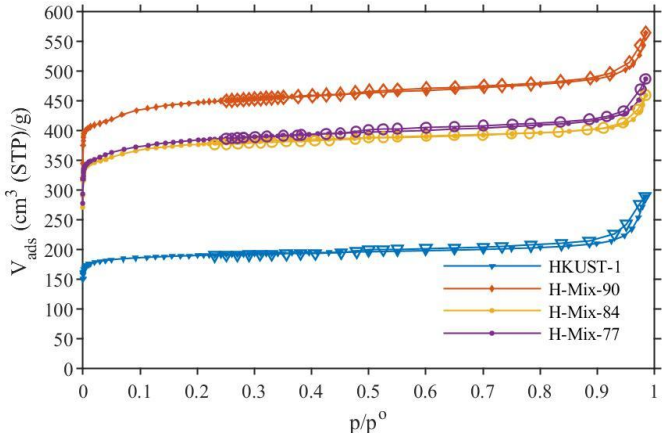

Fig. 7. Adsorption (solid markers)- desorption isotherms for HKUST-1 and H-Mix-XX MOFs

TABLE 2
TEXTURAL PROPERTIES OF MATERIALS

MOF	Specific area (m^2/g)	Micropore volume (cm^3/g)	Total pore volume (cm^3/g)
HKUST-1	770	0.29	0.43
H-Mix-90	1750	0.64	0.84
H-Mix-84	1500	0.58	0.68
H-Mix-77	1500	0.56	0.68

The reduced N_2 adsorption in HKUST-1, compared to mixed ligand materials, is likely due to structural defects, such as missing PW nodes or incomplete ligand coordination, as reported in analogous systems [14], [15], [28]. Nevertheless, these defects may also enhance the N_2 adsorption by generating OMS. With fewer carboxylates per ligand, iBDC unsaturated Cu^{2+} sites are created, strengthening quadrupolar interactions with N_2 [13].

The excess hydrogen adsorption at 77 K (Fig. 8) follows the trend observed for nitrogen adsorption shown in Fig.5: the highest adsorption occurs for the H-Mix90 material, reaching a value of 440 cm^3 H_2/g MOF at 8 bar. Meanwhile, the solids H-Mix-84 and H-Mix77, which have a higher proportion of substituted original ligands, exhibit lower adsorption than H-Mix-90, with a 350 cm^3 H_2/g MOF value. The fact that the amount of adsorbed hydrogen does not increase as BTC is replaced and more OMS are formed can be attributed to the convolution of two effects: the increase in adsorption potential due to the quadrupole moment of hydrogen and the reduction in micropore size and specific surface area [13].

According to seveal studies, the H-MiX90 performs well at 77 K and 1 bar, even when compared with materials obtained with traditional methods (e.g., solvothermal), as shown in Table 3.

Energy density (E_D) of H-Mix-90 at 8 bar and 77 K, was calculated using (2):

$$E_D = \frac{V_{ads} \cdot H_{H_2}}{0.881 \cdot 22.4 \cdot 1000} \qquad (2)$$

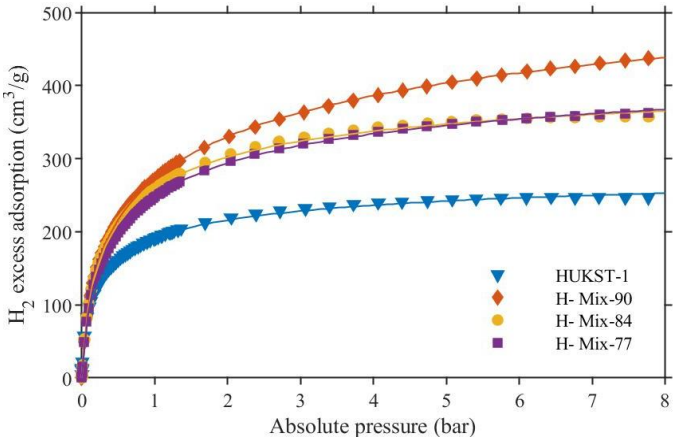

Fig. 8. Excess H_2 adsorption isotherms at 77 K for synthesized MOFs. The continuous line corresponds to Tóth model fitting.

TABLE 3
COMPARISON OF MATERIAL PERFORMANCE WITH PREVIOUSLY REPORTED MOFS

Material	H_2 uptake (77K – 1 bar) cm^3/g	Approach	Synthesis method
H-Mix-90	271	Mixed ligands (This work)	Mecanochemical
Zn- CuBTC	181	Mixed metals [29]	Solvothermal
Li-d-HKUST-1	275	Mixed ligands + Li dope [28]	Spray
SSC-1-91	272	Mixed ligands [13]	Solvothermal

Where V_{ads} is the hydrogen adsorbed volume in cm^3/g, H_{H2} is its combustion enthalpy assumed as 241.595 kJ/mol [30] 0.881 is the crystallographic density of MOFs, assumed as the one of HKUST-1 and 22.4 is the volume of an ideal gas at standard conditions. The result was 3.3 MJ/L, several times the STP's energy density. Although this value is still far from that of gasoline, the pressure used in this study is significantly lower than the typical pressures for medium-scale storage (100 bar)[31].

Another essential aspect is economic feasibility: a material for hydrogen storage must also be cost-effective. According to DeSantis[32], nearly 50% of the synthesis cost of HKUST-1 is attributed to the ligand. Since iBDC is approximately 20 times cheaper than BTC [33], [34], substituting BTC with iBDC leads to significant cost savings.

IV. Conclusion

This study demonstrates that incorporating mixed ligands in HKUST-1 significantly alters adsorption behaviour and, consequently, its energy storage performance by modulating porosity and the availability of open metal sites. These findings offer valuable insights into the tunability of MOFs for gas storage applications and underscore the potential of ligand engineering as an effective strategy in porous materials. Furthermore, the partial substitution of BTC with iBDC enhances adsorption performance and significantly reduces material costs, making this approach more feasible for large-scale implementation. The economic advantage of replacing BTC with a cheaper alternative, without compromising structural integrity or adsorption performance, further highlights ligand engineering as a cost-effective and scalable strategy for developing MOFs tailored for hydrogen applications. Additionally, the mechanochemical synthesis method employed in this study presents a notable advantage over traditional solvothermal methods by eliminating the need for hazardous solvents, thereby improving safety, reducing environmental impact, and increasing sustainability. The findings reinforce the viability of mechanochemistry as a green, energy-efficient technique for MOF design, paving the way for developing next-generation porous materials for hydrogen storage and beyond.

Acknowledgment

The authors sincerely appreciate the financial support provided by *Universidad Tecnológica Nacional - Facultad Regional Delta*, which made the presentation of this work possible. Their support has been instrumental in sharing these research findings.

References

[1] P. J. Linstrom and W. G. Mallard, *NIST Chemistry WebBook, NIST Standard Reference Database Number 69*. Gaithersburg MD, 20899: National Institute of Standards and Technology, 2018. Accessed: Oct. 29, 2018. [Online]. Available: https://doi.org/10.18434/T4D303

[2] Advanced Research Project Agency −, "Methane Opportunities for Vehicular Energy (MOVE)." Accessed: Jan. 16, 2024. [Online]. Available: https://arpa-e.energy.gov/sites/default/files/documents/files/MOVE_ProgramOverview.pdf

[3] U. Bossel and B. Eliasson, "Hydrogen Economy," 2003.

[4] U. Eberle, M. Felderhoff, and F. Schüth, "Chemical and Physical Solutions for Hydrogen Storage," *Angew. Chem. Int. Ed.*, vol. 48, no. 36, pp. 6608–6630, Aug. 2009, doi: 10.1002/anie.200806293.

[5] J. Ren, H. W. Langmi, B. C. North, and M. Mathe, "Review on processing of metal-organic framework (MOF) materials towards system integration for hydrogen storage: Review on processing of MOF materials towards system integration," *Int. J. Energy Res.*, vol. 39, no. 5, pp. 607–620, Apr. 2015, doi: 10.1002/er.3255.

[6] M. P. Suh, H. J. Park, T. K. Prasad, and D.-W. Lim, "Hydrogen Storage in Metal–Organic Frameworks," *Chem. Rev.*, vol. 112, no. 2, pp. 782–835, Feb. 2012, doi: 10.1021/cr200274s.

[7] K. Momma and F. Izumi, "VESTA 3 for three-dimensional visualization of crystal, volumetric and morphology data," *J. Appl. Crystallogr.*, vol. 44, no. 6, pp. 1272–1276, 2011.

[8] S. S.-Y. Chui, S. M.-F. Lo, J. P. Charmant, A. G. Orpen, and I. D. Williams, "A chemically functionalizable nanoporous material $[Cu_3(TMA)_2\ (H2O)_3]_2$," *Science*, vol. 283, no. 5405, pp. 1148–1150, 1999, doi: 10.1126/science.283.5405.1148.

[9] V. Krungleviciute *et al.*, "Argon Adsorption on Cu_3 (Benzene-1,3,5-tricarboxylate) $_2$ (H_2O) $_3$ Metal−Organic Framework," *Langmuir*, vol. 23, no. 6, pp. 3106–3109, Mar. 2007, doi: 10.1021/la061871a.

[10] M. F. Ghazvini, M. Vahedi, S. N. Nobar, and F. Sabouri, "Investigation of the MOF adsorbents and the gas adsorptive separation mechanisms," *J. Environ. Chem. Eng.*, vol. 9, no. 1, p. 104790, 2021.

[11] Q. Yang and C. Zhong, "Understanding hydrogen adsorption in metal−organic frameworks with open metal sites: a computational study," *J. Phys. Chem. B*, vol. 110, no. 2, pp. 655–658, 2006.

[12] S. Lowell, J. E. Shields, M. A. Thomas, and M. Thommes, *Characterization of Porous Solids and Powders: Surface Area, Pore Size and Density*, vol. 16. in Particle Technology Series, vol. 16. Dordrecht: Springer Netherlands, 2012. doi: 10.1007/978-1-4020-2303-3.

[13] P. S. Gauna *et al.*, "Influence of defect engineering on the hydrogen and methane adsorption capacity in HKUST-1–like structure MOF," *Adsorption*, vol. 29, no. 7, pp. 351–361, 2023.

[14] G. Barin, V. Krungleviciute, O. Gutov, J. T. Hupp, T. Yildirim, and O. K. Farha, "Defect Creation by Linker Fragmentation in Metal–Organic Frameworks and Its Effects on Gas Uptake Properties," *Inorg. Chem.*, vol. 53, no. 13, pp. 6914–6919, Jul. 2014, doi: 10.1021/ic500722n.

[15] W. Zhang *et al.*, "Impact of Synthesis Parameters on the Formation of Defects in HKUST-1: Impact of Synthesis Parameters on the Formation of Defects in HKUST-1," *Eur. J. Inorg. Chem.*, vol. 2017, no. 5, pp. 925–931, Feb. 2017, doi: 10.1002/ejic.201601239.

[16] M. Köberl, M. Cokoja, W. A. Herrmann, and F. E. Kühn, "From molecules to materials: Molecular paddle-wheel synthons of macromolecules, cage compounds and metal–organic frameworks," *Dalton Trans.*, vol. 40, no. 26, p. 6834, 2011, doi: 10.1039/c0dt01722a.

[17] J. Villarroel-Rocha, D. Barrera, J. J. Arroyo-Gómez, and K. Sapag, "Critical Overview of Textural Characterization of Zeolites by Gas Adsorption," in *New Developments in Adsorption/Separation of Small Molecules by Zeolites*, vol. 184, S. Valencia and F. Rey, Eds., in Structure and Bonding, vol. 184. , Cham: Springer International Publishing, 2020, pp. 31–55. doi: 10.1007/430_2020_69.

[18] F. Rouquerol, J. Rouquerol, K. S. W. Sing, P. L. Llewellyn, and G. Maurin, *Adsorption by powders and porous solids: principles, methodology and applications*, Second edition. Amsterdam: Elsevier/AP, 2014.

[19] T. D. Claridge, *High-resolution NMR techniques in organic chemistry*, vol. 27. Elsevier, 2016.

[20] S. M. Cohen, "Postsynthetic Methods for the Functionalization of Metal–Organic Frameworks," *Chem. Rev.*, vol. 112, no. 2, pp. 970–1000, Feb. 2012, doi: 10.1021/cr200179u.

[21] N. C. Burtch, H. Jasuja, and K. S. Walton, “Water stability and adsorption in metal–organic frameworks,” *Chem. Rev.*, vol. 114, no. 20, pp. 10575–10612, 2014.
[22] T. Friščić, C. Mottillo, and H. M. Titi, “Mechanochemistry for Synthesis,” *Angew. Chem. Int. Ed.*, vol. 59, no. 3, pp. 1018–1029, Jan. 2020, doi: 10.1002/anie.201906755.
[23] J. M. Castillo, T. J. H. Vlugt, and S. Calero, “Understanding Water Adsorption in Cu−BTC Metal−Organic Frameworks,” *J. Phys. Chem. C*, vol. 112, no. 41, pp. 15934–15939, Oct. 2008, doi: 10.1021/jp806363w.
[24] M. Thommes *et al.*, “Physisorption of gases, with special reference to the evaluation of surface area and pore size distribution (IUPAC Technical Report),” *Pure Appl. Chem.*, vol. 87, no. 9–10, pp. 1051–1069, 2015.
[25] H. Yang, S. Orefuwa, and A. Goudy, “Study of mechanochemical synthesis in the formation of the metal–organic framework Cu3(BTC)2 for hydrogen storage,” *Microporous Mesoporous Mater.*, vol. 143, no. 1, pp. 37–45, Aug. 2011, doi: 10.1016/j.micromeso.2011.02.003.
[26] W. Yuan *et al.*, “Study of the mechanochemical formation and resulting properties of an archetypal MOF: Cu3(BTC)2 (BTC = 1,3,5-benzenetricarboxylate),” *CrystEngComm*, vol. 12, no. 12, p. 4063, 2010, doi: 10.1039/c0ce00486c.
[27] M. Klimakow, P. Klobes, A. F. Thünemann, K. Rademann, and F. Emmerling, “Mechanochemical Synthesis of Metal−Organic Frameworks: A Fast and Facile Approach toward Quantitative Yields and High Specific Surface Areas,” *Chem. Mater.*, vol. 22, no. 18, pp. 5216–5221, Sep. 2010, doi: 10.1021/cm1012119.
[28] M. Kubo, T. Matsumoto, and M. Shimada, “Enhancement of Hydrogen Adsorption on Spray-Synthesized HKUST-1 via Lithium Doping and Defect Creation,” *Materials*, vol. 16, no. 15, p. 5416, 2023.
[29] A. M. P. Peedikakkal and I. H. Aljundi, “Mixed-Metal Cu-BTC metal–organic frameworks as a strong adsorbent for molecular hydrogen at low temperatures,” *ACS Omega*, vol. 5, no. 44, pp. 28493–28499, 2020.
[30] R. H. Perry, D. W. Green, and J. O. Maloney, “Manual del Ingeniero Quimico, Tomo I,” vol. 333, no. 339, España,: McGraw-Hill.;, p. 738, 1990.
[31] A. Franco and C. Giovannini, “Hydrogen Gas Compression for Efficient Storage: Balancing Energy and Increasing Density,” *Hydrogen*, vol. 5, no. 2, pp. 293–311, May 2024, doi: 10.3390/hydrogen5020017.
[32] D. DeSantis, J. A. Mason, B. D. James, C. Houchins, J. R. Long, and M. Veenstra, “Techno-economic Analysis of Metal Organic Frameworks for Hydrogen and Natural Gas Storage,” *Energy Fuels*, vol. 31, no. 2, pp. 2024–2032, Feb. 2017, doi: 10.1021/acs.energyfuels.6b02510.
[33] Chemfine International Co., Ltd., “Trimesic acid cost,” Alibaba. Accessed: May 05, 2024. [Online]. Available: https://spanish.alibaba.com/p-detail/CAS-1700002901961.html?spm=a2700.galleryofferlist.normal_offer.d_price.114274ccA0hVZi
[34] Hebei Suna Technology Co., Ltd., “Isophthalic acid cost,” Alibaba. Accessed: May 05, 2024. [Online]. Available: https://spanish.alibaba.com/product-detail/Best-Price-Industrial-Grade-Pia-CAS-1601117538769.html?spm=a2700.7724857.0.0.30286c7fXJogdP